Publishing House
AKAPIT

COMPUTER METHODS IN MATERIALS SCIENCE
Informatyka w Technologii Materiałów

Vol. 18, 2018, No. 1

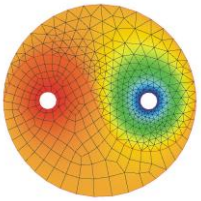

NONLINEAR DYNAMIC ANALYSIS OF AN AXIALLY MOVING POROUS FG PLATE SUBJECTED TO A LOCAL FORCE WITH KINETIC DYNAMIC RELAXATION METHOD

MOSTAFA ESMAEILZADEH[1], MEHRAN KADKHODAYAN[2*]

[1]Department of Mechanical Engineering, Mashhad Branch, Islamic Azad University, Mashhad, Iran
[2]Department of Mechanical Engineering, Ferdowsi University of Mashhad, Mashhad, Iran
**Corresponding author: kadkhoda@um.ac.ir*

Abstract

In some engineering applications like moving ships the axially moving FG structures have to be investigated. In this paper, the nonlinear response and stability of an axially moving porous FGM plate under a local concentrated load are studied. The plate is made of materials whose properties are assumed to be graded in the thickness direction. To take the effect of porosity into account, the modified rule of mixture is chosen to calculate the effective material properties. The kinetic dynamic relaxation method along with the implicit Newmark integration are used to solve the nonlinear dynamic equations. Finally, the effect of material gradient index, porosity volume fraction and boundary conditions on dynamic deflection and instability of plate are discussed.

Key words: Solidification, Binary alloy, Material shrinkage, Immune algorithm

1. INTRODUCTION

In recent years, functionally graded materials (FGMs) have been practiced in industry, particularly in environments with very high temperatures as well as high mechanical loads such as turbines and components of powerful machines. Due to the unique characteristics of these materials, it is anticipated that their industrial applications will be developed over the coming years. These materials for the first time were introduced in 1984 in the laboratory of the Japan Aerospace. Then they have attracted intensive research interests, which were mainly focused on their static, dynamic and vibration characteristics of FG structures (Golmakani & Kadkhodayan, 2013; Fallah & Aghdam, 2012). To produce FGMs, there are different methods such as Powder Metallurgy (Kieback et al., 2003), multi-step sequential infiltration technique, non-pressure sintering technique and self-propagating high temperature synthesis technique (Wang & Zu, 2017). However, porosities or micro-voids can happen inside the FGMs due to the existence of some technical issues during the process. Porosity gradients may be formed either by the deposition of powder mixtures with different particle shape or by varying the deposition parameters including the use of space holders (Kieback et al., 2003). Wattanasakulpong et al. (2012) reported that when the multi-step sequential infiltration technique is applied, porosities happen mainly in the middle zone of the FGMs. The reason is that the penetration of the secondary material into the middle zone is difficult. Nevertheless, infiltrating the material into the top and bottom zones is easier, leading to less porosities in these two zones. Furthermore, porosities can occur within the materials during the process of sintering. This is because of the large difference in solidification temperatures between material constituents (Wattanasakulpong & Ungbhakorn, 2014).

Some studies have been performed on the static and dynamic behavior of porous structures. Among

ISSN 1641-8581

them, Biot (1964) proposed the poroelasticity theory by introducing the bulk dynamic and kinematic variables. In another study, Jabbari et al. (2013) analyzed buckling of radially solid circular plate made of porous material. They assumed a function for changes of porosity distributions through the thickness of the plate. Joubaneh et al. (2014) studied on thermal buckling analysis of porous circular plate bounded with piezoelectric sensor-actuator patch. Wattanasakulpong and Chaikittiratana (2015) modified the rule of mixture to take porosities into consideration in their investigation of free vibration of FG beams. On the basis of Timoshenko theory, Chen and Jang (2015) studied the effect of porosity on buckling of shear beam. To do this, the Ritz method was employed to obtain the critical buckling loads and transverse bending deflections. Recently, Atmane and Tounsi (2015) studied the effect of thickness stretching and porosity on mechanical response of a functionally graded beam resting on an elastic foundation. They found the fundamental frequencies by solving the results of eigenvalue problems. Newly, Ebrahimi et al. (2016) analytically investigated the thermal effects on vibration behavior of temperature-dependent porous functionally graded Euler beams.

Axially moving plates can be met in many industrial applications such as moving ships, aircrafts, automobiles, production of paper, steel, or textiles, and also printing process. Because of its great importance, vibration and dynamic stability of axially moving plates have received considerable attention in recent years. The first dynamic analysis of the plate model of the band saw blade was reported by Ulsoy and Mote (1982). Shin et al. (2005) studied the stability of out-of-plane vibrations of axially moving rectangular membranes. Marynowski and Kapitaniak (2002) studied the effects of axially travelling speed and the internal damping on dynamical stability of two-dimensional axially moving web in details. Nonlinear free vibration of an axially moving beam was investigated by Chen and Yong (2007). They obtained the nonlinear frequencies of two models by the method of multiple scales modes. Hatami and Ronagh (2008) analyzed numerically the free vibration of axially moving viscoelastic plates. They used the rheological models to model the viscoelastic behavior of material. By investigating the instability of an axially moving rectangular plate, Banichuk et al. (2010) depicted that the onset of instability occurred in a divergence form for some critical value of the transport velocity when the frequency of the plate vibrations was equal to zero. The steady laminar boundary layer flow over a moving plate in a moving fluid with convective surface boundary condition and in the presence of thermal radiation was investigated by Ishak et al. (2011). Yang et al. (2012) investigated the stability and nonlinear vibration of an axially moving plate using the finite difference method. Based on Kirchhoff-Love plate theory and linear potential follow model, Yao et al. (2016) investigated dynamics and stability of an axially moving plate interacting with surrounding airflow.

To the best of knowledge of authors, there are no previous studies endeavored to perform the dynamic response of a moving functionally graded porous plate subjected to a concentrated load. In this work, elastic properties of FGM plate are supposed to vary through the thickness direction according to the modified mixture-law form. The nonlinear equations of motion are formulated through the Hamilton's principle on the basis of von Karman relations as well as classic plate theory and then, they are solved by hybrid kinetic dynamic relaxation-Newmark method. As a final point, the effect of different parameters such as boundary conditions, the velocity of plate, the material gradient property (p) and also the porosity volume fraction on transient deflection and stability of the plate are investigated.

2. FGM PLATES WITH POROSITIES

A porous plate of thickness h, width b and length a in a Cartesian coordinate system is shown in figure 1. As depicted, the plate is moving with axial speed, v_p, in the opposite direction of x and a fixed concentrated force, F, is applied on the mid-width of the plate in the transverse direction. Furthermore, the Cartesian coordinate is assumed to lie on the mid-plane of the plate and the effective material properties vary functionally from bottom (metal) to top (ceramic).

When porosities are distributed evenly among the metal and ceramic phases of FGM structures, the modified rule of mixture can be proposed as (Wattanasakulpong & Ungbhakorn, 2014)

$$P = P_m\left(V_m - \frac{\alpha_p}{2}\right) + P_c\left(V_c - \frac{\alpha_p}{2}\right) \tag{1}$$

In equation (1) and hereafter, α_p, subscripts *c* and m are used to indicate the porosity volume fraction, ceramic and metal, respectively. It should be noticed that $\alpha_p << 1$ (Wattanasakulpong & Ungbhakorn, 2014). Moreover, V_c and V_m are the ceramic and metal volume fractions, respectively, which are related by

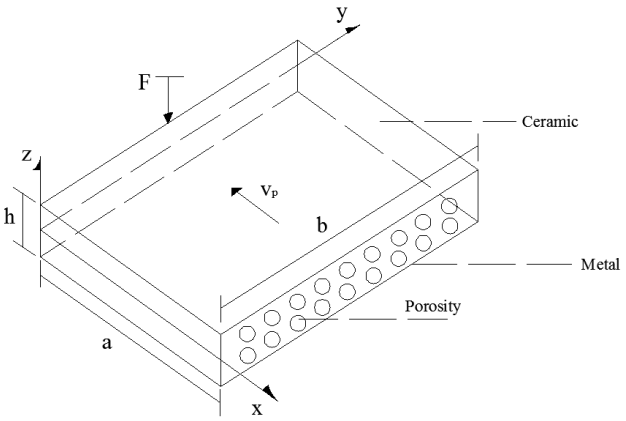

Fig. 1. *Geometry of a FGM plate with porosities.*

$$V_m + V_c = 1 \tag{2}$$

The ceramic volume fraction V_c is assumed to follow a power law distribution as

$$V_c = \left(\frac{2z+h}{2z}\right)^p \tag{3}$$

where *z* is the distance from the mid-plane of the FG plate and volume fraction index or power law *p* dictates the variation of the constituents through the plate thickness. Therefore, all properties of the porous FGM can be written as:

$$P = \left(P_c - P_m\right)\left(\frac{z}{h}+\frac{1}{2}\right)^p + P_m - \frac{\alpha_p}{2}\left(P_c + P_m\right) \tag{4}$$

Thus, the elastic modulus, *E*, and material density, *ρ*, equations of the porous FGM plate can be obtained as

$$\begin{aligned} E(z) &= \left(E_c - E_m\right)\left(\frac{z}{h}+\frac{1}{2}\right)^p + E_m - \frac{\alpha_p}{2}\left(E_c + E_m\right) \\ \rho(z) &= \left(\rho_c - \rho_m\right)\left(\frac{z}{h}+\frac{1}{2}\right)^p + \rho_m - \frac{\alpha_p}{2}\left(\rho_c + \rho_m\right) \end{aligned} \tag{5}$$

The Poisson's ratio, ϑ, is assumed to be constant.

3. DERIVATION OF THE GOVERNING EQUATIONS

In accordance with the von-Karman large deflection theory, strain-displacement relations for the classical thin plate can be expressed as follows

$$\begin{Bmatrix} \bar{\varepsilon}_{xx} \\ \bar{\varepsilon}_{yy} \\ \bar{\varepsilon}_{xy} \end{Bmatrix} = \begin{Bmatrix} u_{,x} + w_{,x}^2/2 - z w_{,xx} \\ v_{,y} + w_{,y}^2/2 - z w_{,yy} \\ u_{,y} + v_{,x} + w_{,x} w_{,y} - 2z w_{,xy} \end{Bmatrix} \tag{6}$$

where *u*, *v* and *w* are the displacement of the mid-plane in the direction of *x*, *y* and *z*, respectively, and the subscript (,) shows the derivative operator with respect to the displacement. Based on Hook's law, the relationships between stress and strain for porous FG plates may be achieved as

$$\begin{Bmatrix} \sigma_{xx} \\ \sigma_{yy} \\ \sigma_{xy} \end{Bmatrix} = \begin{bmatrix} E(z) & \vartheta E(z) & 0 \\ \vartheta E(z) & E(z) & 0 \\ 0 & 0 & \dfrac{E(z)}{2(1+\vartheta)} \end{bmatrix} \begin{Bmatrix} \bar{\varepsilon}_{xx} \\ \bar{\varepsilon}_{yy} \\ \bar{\varepsilon}_{xy} \end{Bmatrix} \tag{7}$$

Using the Hamilton's principle, the equations of motion in the fixed coordinate (*x*, *y*, and *z*) can be derived as

$$\int_0^T \left(\delta U + \delta W - \delta T_k\right) dt = 0 \tag{8}$$

where *U* is the total potential energy of the system, T_k is kinetic energy of the system, *W* is the work performed by external forces and δ is the variation operator. Also, the virtual potential (strain) energy can be written in terms of stress and strain as

$$\delta U = \int_V \delta u dV = \int_V \sigma_{ij} \bar{\varepsilon}_{ij} dV \tag{9}$$

The velocity vector of the axially moving thin plate can be given as (Swope & Ames, 1963)

$$V = \left(C + C\frac{\partial u}{\partial x} + \frac{\partial u}{\partial t}\right) i + \left(C\frac{\partial v}{\partial x} + \frac{\partial v}{\partial t}\right) j + \left(C\frac{\partial w}{\partial x} + \frac{\partial w}{\partial t}\right) k \tag{10}$$

in which *C* is a constant velocity of the plate equal to $-v_p$.

Because the influence of the angles ($w_{,x}$) and ($w_{,y}$) on the velocity vector are negligible, the total kinetic energy T_k is obtained as:

$$\delta T_k = \frac{1}{2}\int_V \rho(z)\left[\left(C + C\frac{\partial u}{\partial x} + \frac{\partial u}{\partial t}\right)^2 + \left(C\frac{\partial v}{\partial x} + \frac{\partial v}{\partial t}\right)^2 + \left(C\frac{\partial w}{\partial x} + \frac{\partial w}{\partial t}\right)^2\right]dV \quad (11)$$

and the virtual work is

$$\delta W = \int_A F\bar{\delta}\left(x - x_0\right)\left(y - y_0\right)\delta w dA \quad (12)$$

The term $\bar{\delta}$ is Dirac delta function, integral of which is equal to unity in any neighborhood of $[x_0, y_0]$ and zero elsewhere (Taheri & Ting, 1989). Moreover, δw and F can be considered as an admissible virtual displacement in z direction and a concentrated constant force subjected on the plate, respectively. The final forms of equilibrium equations are presented as

$$\begin{aligned} &N_{xx,x} + N_{xy,y} = I_0\frac{D^2u}{Dt^2} \\ &N_{xy,x} + N_{yy,y} = I_0\frac{D^2v}{Dt^2} \\ &M_{xx,xx} + 2M_{xy,xy} + M_{yy,yy} + \mathcal{N} + F\bar{\delta}\left[(x-x_0)(y-y_0)\right] = I_0\frac{D^2w}{Dt^2} \\ &\mathcal{N} = N_{xx}w_{,xx} + 2N_{xy}w_{,xy} + N_{yy}w_{,yy} \end{aligned} \quad (13)$$

where:

$$I_0 = \int_{-h/2}^{h/2}\rho(z)dz \quad (14)$$

$$\frac{D^2}{Dt^2} = \frac{\partial^2}{\partial t^2} + 2C\frac{\partial^2}{\partial x \partial t} + C^2\frac{\partial^2}{\partial x^2} \quad (15)$$

3.1 Plate boundary conditions

The boundary conditions used in present study are presented as follows

a) For simply supported boundary condition (SSSS):

$$\begin{cases} x = 0, a \rightarrow u = v = w = M_{xx} = 0 \\ y = 0, b \rightarrow u = v = w = M_{yy} = 0 \end{cases} \quad (16)$$

b) For clamped boundary condition (CCCC):

$$\begin{cases} x = 0, a \rightarrow u = v = w = w_{,x} = 0 \\ y = 0, b \rightarrow u = v = w = w_{,y} = 0 \end{cases} \quad (17)$$

c) For SCSC (parallel edges are in the same conditions):

$$\begin{cases} x = 0, a \rightarrow u = v = w = M_{xx} = 0 \\ y = 0, b \rightarrow u = v = w = w_{,y} = 0 \end{cases} \quad (18)$$

4. SOLUTION OF THE PROBLEM

In this section, the Newmark method has been used to discretize the equations in time domain. To solve the dynamic equations, however, the Newmark method needs to be combined by a common nonlinear solver such as Newton-Raphson or dynamic relaxation. In this study, due to simplicity, efficiency and unique procedure for both linear and nonlinear systems, the kinetic dynamic relaxation method has been adopted.

4.1 Implicit Newmark method

According to the Newmark approach, the real acceleration and velocity at the next time step (j+1) can be computed by equations (19) and (20) (Clough & Penzien, 1993) as

$$\boldsymbol{a}_{j+1} = \frac{1}{\beta(\Delta t_j)^2}\Delta\boldsymbol{x}_j - \frac{1}{\beta\Delta t_j}\boldsymbol{a}_j - \left(\frac{1}{2\beta} - 1\right)\boldsymbol{a}_j \quad (19)$$

$$\boldsymbol{v}_{j+1} = \frac{\gamma}{\beta\Delta t_j}\Delta\boldsymbol{x}_j - \left(\frac{\gamma}{\beta} - 1\right)\boldsymbol{v}_j - \left(\frac{\gamma}{2\beta} - 1\right)\Delta t_j\boldsymbol{a}_j \quad (20)$$

in which $\boldsymbol{x}_j$ shows the displacement field of the plate and Δt represents the time interval. Moreover, the constancy and precision of Newmark's responses can be guaranteed by appropriate quantities, namely β and γ. By substituting equations (19) and (20) into equation (13), the dynamic equations can be converted into a static system as

$$\left[\bar{\boldsymbol{K}}_{j+1}\right]\boldsymbol{x}_{j+1} = \{\bar{\boldsymbol{P}}_{j+1}\} \quad (21)$$

where $\left[\bar{\boldsymbol{K}}_{j+1}\right]$ and $\left\{\bar{\boldsymbol{P}}_{j+1}\right\}$ are equivalent stiffness matrix and equivalent load vector, respectively (Rezaiee-Pajand & Alamatian, 2008) and are formulated as

$$\left[\bar{\boldsymbol{K}}_{j+1}\right] = \frac{1}{\beta(\Delta t_j)^2}\left[\boldsymbol{M}_{j+1}\right] + \frac{\gamma}{\beta\Delta t_j}\left[\boldsymbol{C}_{j+1}\right] + \left[\boldsymbol{K}_{j+1}\right] \quad (22)$$

$$\bar{\boldsymbol{P}}_{j+1} = \boldsymbol{P}\left(\mathrm{t}_{j+1}\right) + \begin{Bmatrix} \left[\boldsymbol{M}_{j+1}\right]\left[\frac{1}{\beta(\Delta t_j)^2}\boldsymbol{x}_j + \frac{1}{\beta\Delta t_j}\boldsymbol{v}_j + \left(\frac{1}{2\beta} - 1\right)\boldsymbol{a}_j\right] + \\ \left[\boldsymbol{C}_{j+1}\right]\left[\frac{\gamma}{\beta\Delta t_j}\boldsymbol{x}_j + \left(\frac{\gamma}{\beta} - 1\right)\boldsymbol{v}_j + \left(\frac{\gamma}{2\beta} - 1\right)\Delta t_j\boldsymbol{a}_j\right] \end{Bmatrix} \quad (23)$$

where $\left[\boldsymbol{M}_{j+1}\right], \left[\boldsymbol{C}_{j+1}\right], \left[\boldsymbol{K}_{j+1}\right]$ are, respectively, the mass, damping and stiffness matrices and also $\left\{\boldsymbol{P}(t_{j+1})\right\}$ represents the external force vector. Then

equation (21) may be solved by dynamic relaxation method with kinetic damping technique.

4.2 Kinetic dynamic relaxation method

In this method, to solve the nonlinear equations, equation (21) is transferred to fictitious dynamic space by adding fictitious mass matrix $[\boldsymbol{M}]_{DR}$. Thus, equation (21) is improved as

$$[\boldsymbol{M}]_{DR}^{n}\{\ddot{\boldsymbol{x}}\}^{n}+\left[\bar{\boldsymbol{K}}_{j+1}\right]^{n}\boldsymbol{x}_{j+1}^{n}=\bar{\boldsymbol{P}}_{j+1}^{n} \tag{24}$$

in which $\{\ddot{\boldsymbol{x}}\}$ and symbol n are fictitious acceleration vector and the iteration number, respectively. The mass matrix should be defined in order to guarantee the stability and convergence of the procedure. Based on the Gershgörin theorem, the fictitious mass matrix elements are obtained by following equation (Alamatian, 2012)

$$\boldsymbol{m}_{ii}^{l}\geq\frac{1}{2}\left(\tau^{n}\right)^{2}\sum_{j=1}^{N}|\boldsymbol{k}_{ij}^{l}|,\ l=\boldsymbol{u},\boldsymbol{v},\boldsymbol{w}\qquad \boldsymbol{k}_{ij}=\frac{\partial\left\{[\bar{\boldsymbol{K}}]^{n}x^{n}\right\}}{\partial x} \tag{25}$$

By introducing residual force from

$$\{\boldsymbol{R}\}^{n}=\bar{\boldsymbol{P}}_{j+1}^{n}-\left[\bar{\boldsymbol{K}}_{\boldsymbol{j}+1}\right]^{\boldsymbol{n}}\boldsymbol{x}_{j+1}^{n} \tag{26}$$

nodal velocity and displacement vectors at the next step of fictitious time $\left(\tau^{n}\right)$ can be calculated as

$$\{\dot{\boldsymbol{x}}\}^{\boldsymbol{n}+1/2}=\dot{\boldsymbol{x}}^{\boldsymbol{n}-1/2}+\frac{\tau^{n}}{[\boldsymbol{M}]_{\boldsymbol{DR}}}\{\boldsymbol{R}\}^{\boldsymbol{n}} \tag{27}$$

$$\{\boldsymbol{x}\}^{\boldsymbol{n}+1}=\{\boldsymbol{x}\}^{\boldsymbol{n}}+\tau^{n}\{\dot{\boldsymbol{x}}\}^{\boldsymbol{n}+\frac{1}{2}} \tag{28}$$

Using following equation, the kinetic energy of whole system can be achieved as

$$\boldsymbol{KE}^{\mathbf{n}+1}=\frac{1}{2}\sum_{\mathrm{i}=1}^{N}\boldsymbol{m}_{\mathbf{ii}}^{\mathbf{n}}\left(\boldsymbol{v}_{\mathbf{i}}^{\mathbf{n}+\frac{1}{2}}\right)^{2} \tag{29}$$

where, N is the number of degrees of freedom. The kinetic energy of the system is traced through the time domain and once a peak is distinguished the current velocities are set to zero (Lee et al., 2011; Alic & Persson, 2016). After that, the new iteration of K-DR starts with a new nodal displacement and velocity as (Topping & Ivanyi, 2007)

$$\{\boldsymbol{v}\}^{\boldsymbol{n}+\frac{1}{2}}=\frac{\tau^{n}}{2(\boldsymbol{m}_{\boldsymbol{DR}})_{\boldsymbol{ii}}^{\boldsymbol{n}}}\{\boldsymbol{R}\}^{\boldsymbol{n}} \tag{31}$$

Understandably, the values of velocity vector approach zero at the steady state situation. The K-DR procedure is continued until $\left|\boldsymbol{KE}^{n+1}\right|\leq10^{-9}$ or $\left|\left\{\boldsymbol{R}^{n}\right\}\right|\leq10^{-8}$. These steps are iterated for each time increment of implicit numerical integration.

5. NUMERICAL RESULTS

The transient responses of the moving porous FG plate are obtaiend here by means of the hybrid KDR-Newmark technique. To do this, firstly, the convergence and accuracy of the method is demonstrated by a few samples and then a comprehensive parametric study is presented.

5.1 Validation of present study

Sample 1. As a first example to verify the present formulation and numerical method, the large transient central deflection and moment of a simply supported isotropic rectangular plate subjected to various distributed pulse loads, *q*, are investigated, figure 2. The assumed properties, dimensions and load are assumed as

$$\begin{pmatrix} a=b=2.438m, h=6.35\times10^{-3}m \\ E=69\times10^{9}Pa, \rho=2496\frac{kg}{m^{3}}, \\ \vartheta=0.25 \\ q=47.87\frac{N}{m^{2}} \end{pmatrix} \tag{32}$$

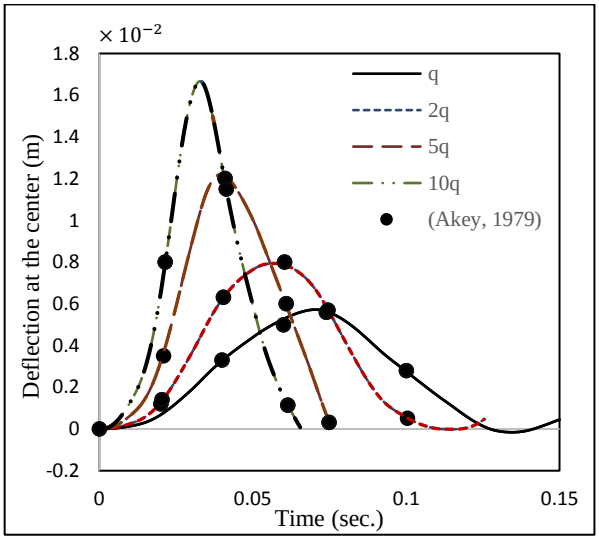

Fig. 2a *Dynamic responses at the center of a SSSS rectangular plate, Deflection.*

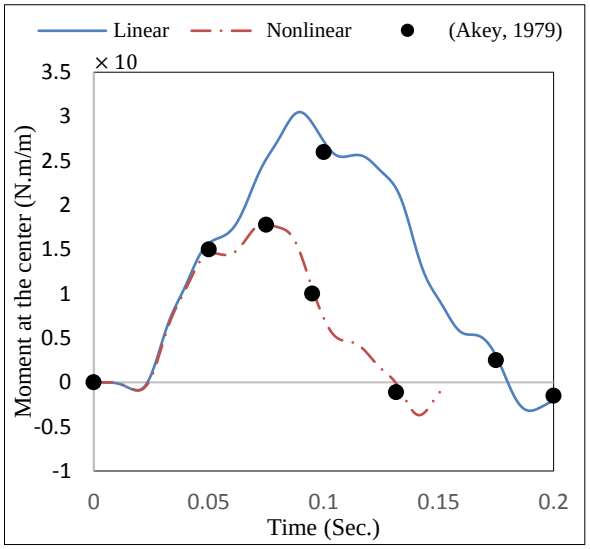

Fig. 2b. *Dynamic responses at the center of a SSSS rectangular plate, Moment.*

The obtained results by KDR are compared with those reported by Akey (1979) and a good agreement between them is observed, figure 2.

Sample 2. In this case, the accuracy and workability of KDR method for moving structures is verified. For this purpose, the obtained numerical results are compared with those achieved by Chen et al. (2011). They investigated dynamic responses of an axially moving beam ($b<<a$) along with the following dimensionless equations

$$w_{tt} + 2vw_{xt} - (1-v^2)w_{xx} + \xi w_{xxxx} = 0$$
$$\xi = \frac{EI}{P_0 a^2}, T = t\sqrt{\frac{P_0}{\rho a^2}} \tag{33}$$

where v is the dimensionless velocity, P_0 the axial tension, EI the flexural rigidity, ρ the mass density of the beam and a the beam length. Furthermore, t and T are time and dimensionless time, respectively.

As seen, figure 3 demonstrates the truthfulness of KDR method for obtaining dimensionless transient responses of a beam moving with the dimensionless velocity of 1 at the center of the moving beam, W(x=1/2), for fully clamped boundary condition.

Sample 3. In the third case study, the validity of kinetic dynamic relaxation for the plate under a local force, is investigated. It is presumed that the motionless plate ($v_p = 0$) is subjected to a moving concentrated load (v_f); then the KDR results for CCCC and SSSS boundary conditions are compared with those obtained by Eftekhari (2014). Figures 4 and 5 illustrate the time history of deflection at the center of the plate subjected to a moving load. A close agreement can be seen between the present results and the reference (Eftekhari, 2014).

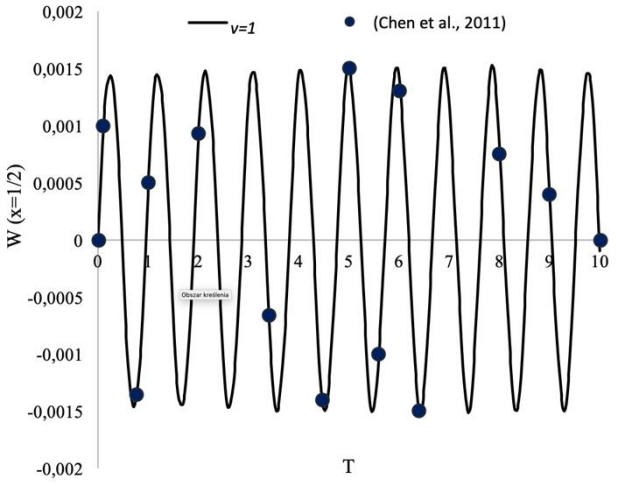

Fig. 3. *Dimensionless deflection at the center of a clamped moving beam in different velocities, $\xi = 0.1$.*

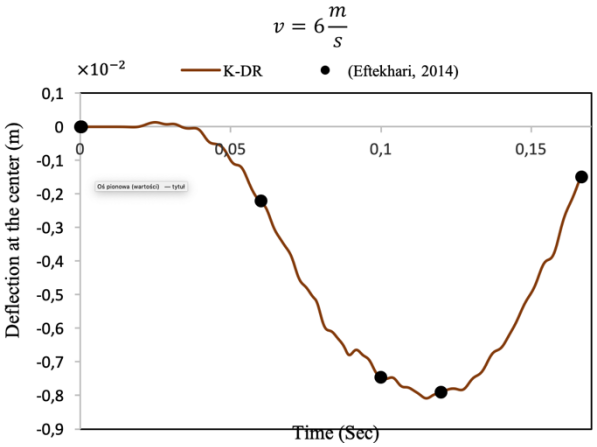

Fig 4. *Comparison of KDR results for central deflection of a CCCC square plate under moving load.*

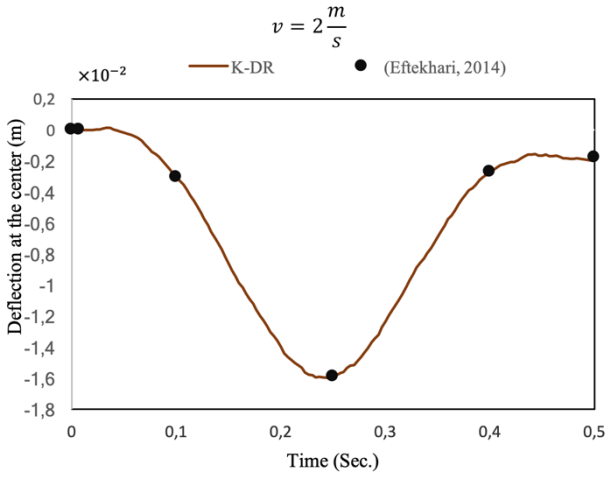

Fig 5. *Central deflection of a SSSS square plate under moving load.*

5.2 Parametric study

An axially moving plate with aspect ratio of a/h=20 (a = 0.1m) is assumed, figure 1. The FGM plate is made from alumina (Al_2O_3) as ceramic and aluminum (Al) as metal; whose material properties are given in table 1.

Table 1. *The mechanical properties of composed materials of FGM plate.*

Material	Elastic module (GPa)	Density (kg/m^3)	Poisson's ratio
Al_2O_3	380	3960	0.3
Al	70	2702	0.3

As aforementioned, the moving plate is subjected to a local concentrated load with amplitude of 100 kN on mid-width of the plate (y = b/2), indeed the fixed load moves on the plate with the velocity of -v_p.

Effect of velocity on the moving plate can be clarified by comparing transient central deflections of a fully clamped pure alumina square plate due to a moving load, v_p =0, with those of a moving plate subjected to a local load for the velocities of 2m/s and 6m/s, figure. 6. When the velocity is low, there is no significant difference between the deflection results obtained from the moving load and moving plate. However, the differences between them become more as the velocity increases.

Figure 7 shows the effect of the material gradient property (index p) on the dynamic responses of a moving porous FGM plate, $\alpha_p = 0.1$, with v_p = 6 m/s in SSSS and CCCC boundary conditions. As depicted, the magnitude of deflection is influenced by the type of boundary conditions and also the value of material gradient property, p. It means that reducing the boundary condition constrains or raising p can increase the magnitude of deflection.

Tables 2 and 3 provide the influence of the FGM index as well as the velocity of the non-porous plate on maximum central deflection and instability for simply supported and clamped boundary conditions, respectively. It can be clearly seen that when the velocity of the plate increase, the central maximum deflection increases initially; however, by increasing the speed of the plate, this deflection decreases until the plate becomes unstable (the deflection approaches to infinity) at critical velocity.

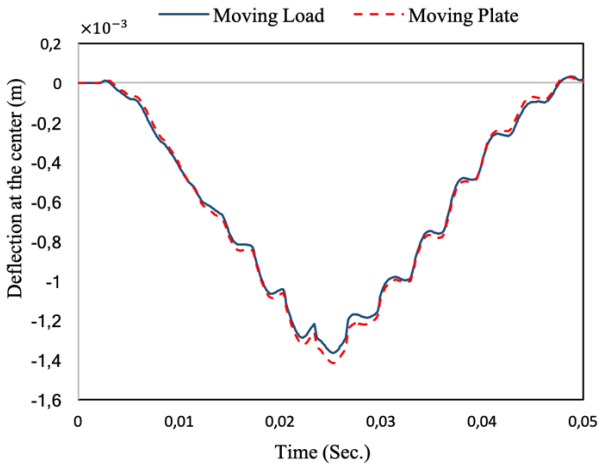

(a)

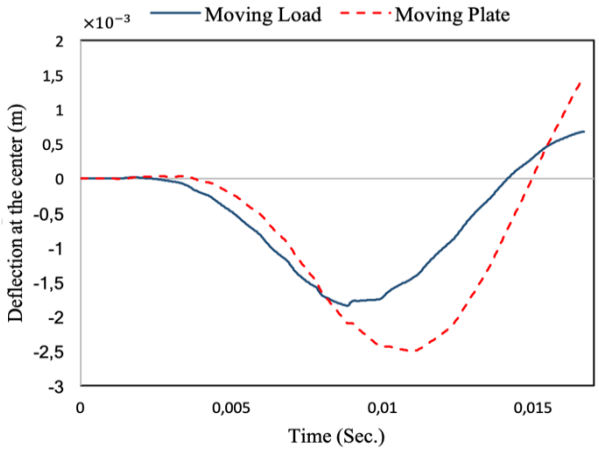

(b)

Fig. 6*. Deflections of the fully clamped square plate for concentrated moving load and moving plate, (a) velocity = 2m/s, (b) velocity = 6m/s.*

As demonstrated, the value of critical velocity can be reduced by softening the FG plate and the growth of degrees of freedom, as well. For example, the non-porous FG plate with p = 0.5 becomes unstable at 21 m/s in CCCC, while it becomes unstable at 20 m/s in SSSS boundary conditions.

The dynamic centroidal deflection of FG plate with various porosity volume fractions and velocity with p = 4 is proposed in tables 4 and 5 for simply supported and clamped boundary conditions, respectively. Comparing the obtained results, it can be found that the dynamic deflection as well as the critical velocity of the plate are strongly influenced by the porosity volume fractions. For instance, the critical velocity of the SSSS plate with $\alpha_p = 0.1$ is 15 m/s while it is 14 m/s for $\alpha_p = 0.2$.

The influence of plate width reduction on dynamic response of the porous plate is shown in figure 8. The velocity of this porous FG plate with p = 1 is 5m/s when SCSC boundary conditions are used. As depicted, by reducing the value of width from 0.1m to 0.075m, the amount of maximum dynamic response decreases as 39.1%, 38.1%, 36.5% and 34% for α_p=0, α_p=0.1, α_p=0.2, α_p=0.3, respectively.

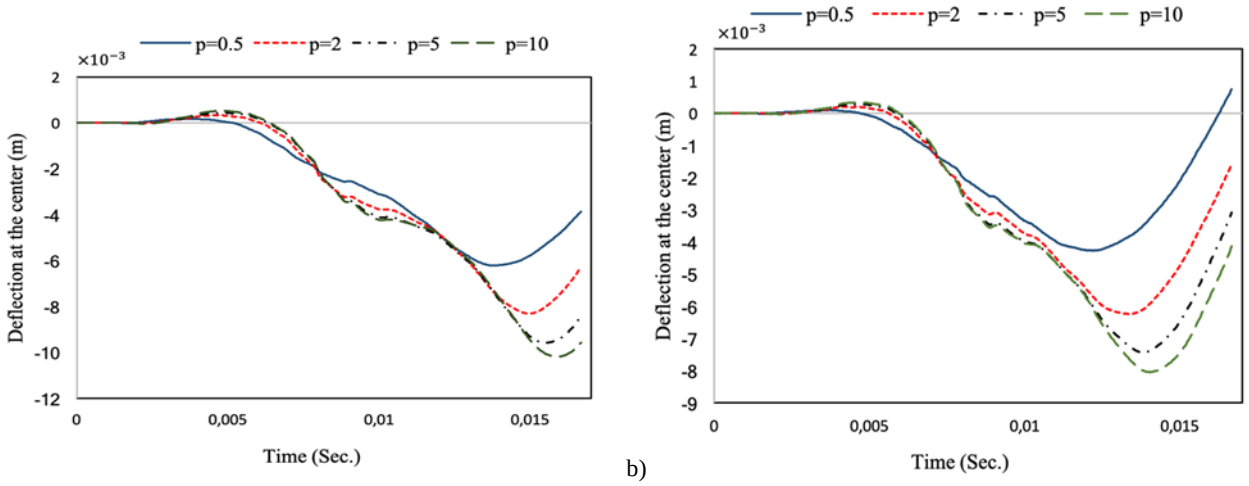

Fig. 7. *Time history of the centroidal defelction of the moving FG square plate subjected to local force, (a) SSSS, (b) CCCC.*

Table 2*. The effect of value of exponent p and velocity of the FG square plate on central maximum deflection* (×10^{-3} m) *for SSSS boundary condition.*

Material	Velocity (m/s)											
p	1	6	7	9	10	12	14	16	17	18	20	21
0.5	-3.84	-6.16	-6.61	-2.02	-1.55	-0.621	-0.604	-1.51	-1.77	-1.5	INF	-
2	-4.85	-7.92	-7.81	-2.61	-1.20	-0.932	-2.59	-0.9	INF	-	-	-
5	-5.95	-8.86	-7.61	-2.71	-0.94	-1.45	-3.48	INF	-	-	-	-

Table 3*. The effect of value of exponent p and velocity of the FG square plate on central maximum deflection* (×10^{-3} m) *for CCCC boundary condition.*

Material	Velocity (m/s)											
p	1	6	7	9	10	12	14	16	17	18	20	21
0.5	-2.16	-4.35	-4.93	-4.24	-1.91	-1.06	-0.588	-0.77	-0.95	-0.1	-0.27	INF
2	-3.64	-6.20	-6.81	-2.38	-2.11	-0.853	-1.48	-1.82	-1.66	INF	-	-
5	-4.21	-7.31	-7.44	-2.54	-2.18	-1.14	-2.5	-3.86	INF	-	-	-

Table 4*. The effect of value of α_p and velocity of the FG square plate on central maximum deflection* (×10^{-3} m) *for SSSS boundary condition* (p = 4).

	Velocity (m/s)								
α_p	**2**	**4**	**6**	**8**	**10**	**12**	**14**	**15**	**16**
0.1	-7	-8.36	-9.2	-3.75	-0.94	-2.90	-2.20	INF	-
0.2	-7.73	-9.08	-9.66	-3.98	-1.78	-3.78	INF	-	-

Table 5. *The effect of value of α_p and velocity of the FG square plate on central maximum deflection* ($\times 10^{-3}$ m) *for CCCC boundary condition* ($p = 4$)**.**

	Velocity (m/s)								
α_p	**2**	**4**	**6**	**8**	**10**	**12**	**15**	**16**	**18**
0.1	-4.73	-6.83	-7.88	-3.46	-1.24	-1.84	-6.57	INF	-
0.2	-5.67	-7.24	-8.502	-3.841	-1.46	-3.12	INF	-	-

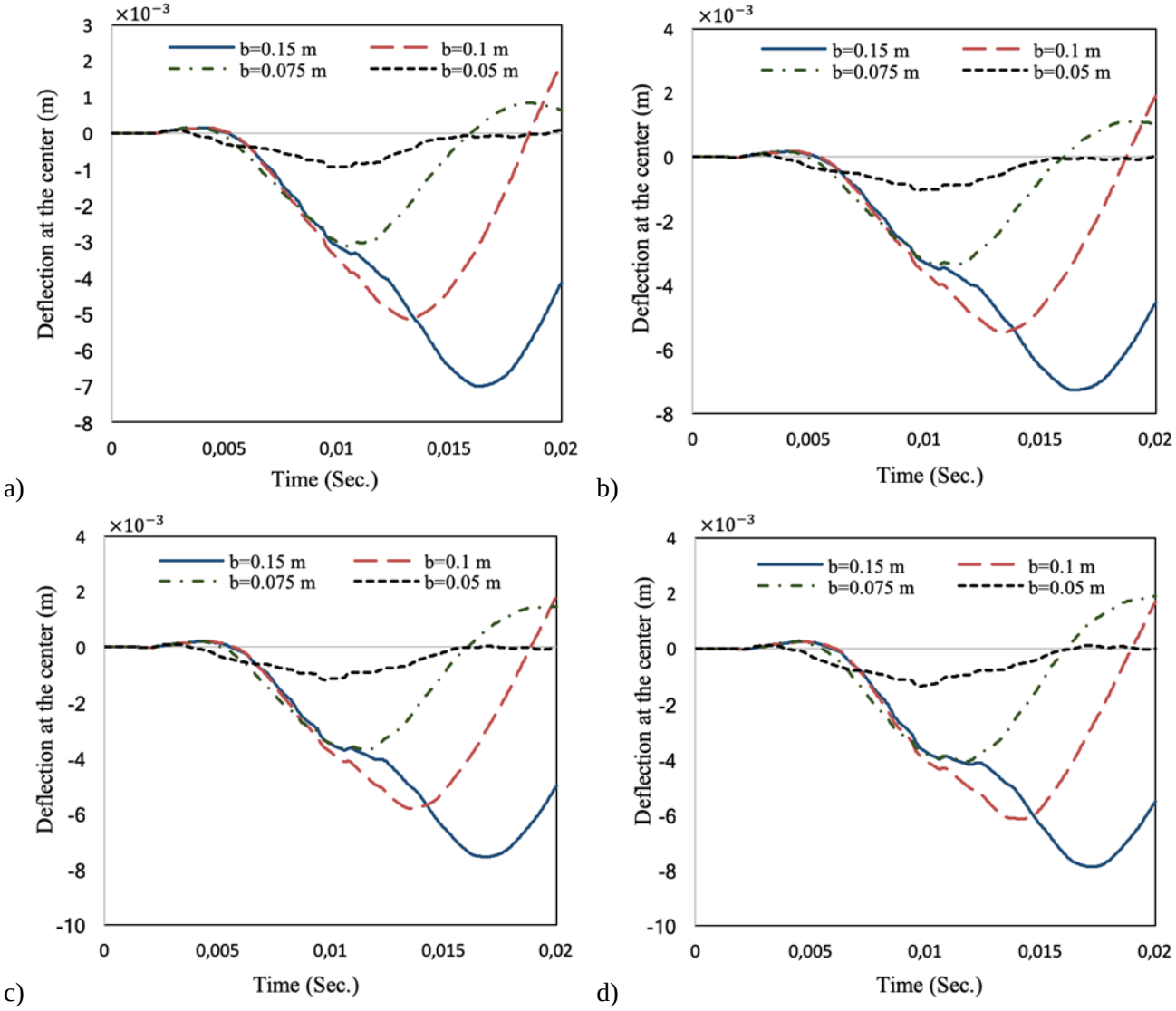

Fig 8*. The effect of width change on dynamic response of the SCSC porous FG plate, v_p = 5m/s, P = 1 (a) α_p = 0, (b) α_p = 0.1, (c) α_p = 0.2 (d) α_p = 0.3.*

6. CONCLUSIONS

In this study, the dynamic responses and stability for an axially porous FG plate for various boundary conditions are investigated. Under classic hypothesis and von-Karman large deflection theory, the nonlinear dynamic equations were derived. The modified rule of mixture covering porosity phases was used to describe and approximate material properties of the porous FGM plates.

Using the new method, kinetic dynamic relaxation technique modified along with Newmark integration, these equations were solved. The effects of the material gradient constant, porosity volume fraction, the velocity of plate, boundary conditions and the width of the plate were investigated in details.

Some vital inferences obtained from parametric study are mentioned as bellow:

- There is no major difference between the results of a moving load and a moving plate, once the velocity of the plate is low. Increasing this velocity; however, the difference between these two results becomes greater which is because of the influence on inertia of the plate.
- Porosity plays a crucial role in instability of moving FG structures. The critical velocity can occur faster by raising porosity volume fraction.
- The influence of width variation on amount of transient response can be increased or decreased by reduction or increasing of α_p, respectively.

CONFLICT OF INTEREST

The authors declare that they have no conflict of interest.

REFERENCES

Akay, H., 1979, Dynamic large deflection analysis of plates using mixed finite elements, *Comput. Struct.*, 11, 1-11.

Alamatian, J., 2012, A new formulation for fictitious mass of the dynamic relxation method with kinetic damping, *Comput. Struct*, 90-91, 42-54.

Alic, V., Persson, K., 2016, Form finding with dynamic relaxation and isogeometric membrane, *Comput. Methods Appl. Mech. Engrg*., 300, 734-747.

Atmane, H., Tounsi, A., Bernard, F., 2015, Effect of thickness stretching and porosity on mechanical response of a functionally graded beams resting on elastic foundations, *Int. J. Mech. Mater. Des.*, 1-14.

Banichuk, N., Jeronen, J., Neittaanmaki, P., Tuovinen, T., 2010, On the instability of an axially moving elastic plate, *Int. J. Solids Struct*., 47, 91-99.

Biot, M., 1964, Theory of buckling of a porous slab and its thermoelastic analogy, *J. Appl. Mech*., 31, 194-198.

Chen, A., Jian, S., 2011, Dynamic response of clamped axially moving beam: integral transform, *Appl. Math. Comput*., 218, 249-256.

Chen, D., Yang, J., Kitipornchai, S., 2015, Elastic buckling and static bending of shear deformable functionally graded porous beam, *Compos. Struct*., 133, 54-61.

Chen, L.-Q., Yang, X.-D., 2007, Nonlinear free transverse vibration of an axially moving beam: comparison of two models, *J. Sound. Vib*., 299, 348-354.

Clough, R., J.Penzien, 1993, *Dynamic of Structures*, s.l.: McGraw-Hill.

Ebrahimi, F., Ghasemi, A., Salari, E., 2016, Investigating thermal effects on vibration behavior of temperature-dependent compositionally graded euler beams with porosities, *Meccanica*, 51, 223-249.

Ebrahimi, F., Zia, M., 2015, Large amplitude nonlinear vibration analysis of functionally graded Timoshenko beams with porosities, *Acta Astronaut*., 116, 117-125.

Eftekhari, S., 2014, A Differential quadrature procedure with regularization of dirac – delta – function for numerical solution of moving load problem, *Lat. Am. J. Solids Struct.*, 12, 1241-1265.

Fallah, A., Aghdam, M., 2012, Thermo-mechanical buckling and nonlinear free vibration analysis of functionally graded beams on nonlinear elastic foundation, *Compos B*., 43, 1523-1530.

Golmakani, M., Kadkhodayan, M., 2013, Large deflection thermoelastic analysis of functionally graded stiffened annular sector plates, *Int. J. Mech. Sci*., 69, 94-106.

Hatami, S., Ronagh, H., Azhari, M., 2008, Exact free vibration analysis of axially moving viscoelastic plates, *Comput. Struct*., 86, 1738–1746.

Ishak, A., Azizah Yacob, N., Bachok, N., 2011, Radiation effects on the thermal boundary layer flow over a moving plate with convective boundary condition, *Meccanica*, 46, 795–801.

Jabbari, M., Joubaneh, E., Khorshidvand, A., Eslami, M., 2013, Buckling analysis of porous circular plate with piezoelectric actuator layers under uniform radial compression, *Int. J. Mech. Sci*., 70, 50-56.

Joubaneh, E., Mojahedin, A., Khorshidvand, A., Jabbari, M., 2014, Thermal buckling analysis of porous circular plate with piezoelectric sensor–actuator layers under uniform thermal load, *J. Sandwich. Struct. Mater*., 17, 3-25.

Kieback, B., Neubrand, A., Riedel, A., 2003, Processing techniques for functionally graded materials, *Mater. Sci. Eng., A*, 362, 81-106.

Lee, K. S., Han, S. E., Park, T., 2011, A simple explicit arc-length method using the dynamic relaxation method, *Comput. Struct*., 89, 216-233.

Marynowski, K., and Kapitaniak, T., 2002, Kelvin-Voigt versus Burgers internal damping in modeling of axially moving viscoelastic web, *Int. J. Non-Linear Mech*., 37, 1147-1161.

Rezaiee-Pajand, M., Alamatian, J., 2008, Nonlinear dynamic analysis by dynamic relaxation method, *J. Struct. Eng. Mech*., 28, 549-570.

Shin, C., Chung, J., Kim, W., 2005, Dynamic characteristics of the out-of-plane vibration for an axially moving membrane, *J. Sound Vib*., 286, 1019-1031.

Swope, R., Ames, W., 1963, Vibration of moving threadline, *J. Franklin Inst*., 275, 36-55.

Taheri, M., Ting, E., 1989, Dynamic response of plate to moving loads: structural impedance method, *Comp. Struct*., 33, 1379-1390.

Topping, B., Ivanyi, P., 2007, *Computer aided design of cable-membrane structures*, s.l.: Saxe-Coburg Publications on Computational Engineering.

Ulsoy, A, Mote Jr., C., 1982, Vibrations of wide band saw blades, *ASME*, 104, 71-78.

Wang, Y.Q., Zu, J.W., 2017, Vibration characteristics of moving sigmoid functionally graded plates containing porosities, *Int. J. Mech. Mater. Des.*, 1-17.

Wattanasakulpong, N., Gangadhara Prusty, B., Kelly, D.W., Hoffman, M., 2012, Free vibration analysis of layered functionally graded beams with experimental validation, *Mater. Des*. 36, 182-190.

Wattanasakulpong, N., Chaikittiratana, A., 2015, Flexural Vibration of imperfect functionally graded beams based on timoshenko beam theory: Chebyshev collocation method, *Meccanica*, 50, 1331-1342.

Wattanasakulpong, N., Ungbhakorn, V., 2014, Linear and nonlinear vibration analysis of elastically restrained ends FGM beams with porosities, *Aerosp. Sci. Tech.*, 1, 111-120.

Yang, X., Zhang, W., Chen, L., Yao, M., 2012, Dynamical analysis of axially moving plate by finite difference method, *Nonlinear Dyn*., 67, 997-1006.

Yao, G., Zhang, Y.-M., 2016, Dynamics and stability of an axially moving plate interacting with surrounding airflow, *Meccanica*, 51, 2111-2119.

NIELINIOWA DYNAMICZNA ANALIZA POROWATEJ PŁYTY FG PORUSZAJĄCEJ SIĘ OSIOWO I PODDANEJ DZIAŁANIU LOKALNEJ SIŁY WYKORZYSTUJĄC METODĘ KINETYCZNO DYNAMICZNEJ RELAKSACJI

Streszczenie

Niektóre inżynierskie problemy, jak na przykład poruszający się okręt, wymagają zastosowania analizy przemieszczających się osiowo struktur gradientowych (ang. Functionally graded materials FGM). W niniejszym artykule opisano badania nieliniowej odpowiedzi i stabilności poruszającej się osiowo porowatej płyty FGM poddanej działaniu lokalnej siły. Płyta była wykonana z materiału, którego własności zmieniały się wzdłuż grubości. Aby uwzględnić wpływ porowatości zastosowano zmodyfikowaną regułę mieszanin, za pomocą której obliczono efektywne własności materiału. Nieliniowe równania dynamiczne zostały rozwiązane za pomocą kinetyczno dynamicznej metody relaksacji połączonej z niejawnym całkowaniem metodą Newmark. W pracy omówiono wpływ gradientu własności, ułamka objętości pustek oraz warunków brzegowych na dynamiczne odkształcenie i niestabilność płyty.

Received: May 9, 2018
Received in a revised form: October 25, 2018
Accepted: November 7, 2018